1966ApJ...143..313S

THREE-COLOR PHOTOMETRY OF THE BRIGHT STARS IN THE GLOBULAR CLUSTER M92

ALLAN SANDAGE AND MERLE F. WALKER*
Mount Wilson and Palomar Observatories
Carnegie Institution of Washington, California Institute of Technology
Received July 26, 1965

ABSTRACT

Three-color photoelectric measurements on the *UBV* system are reported for 71 stars in and near M92 which range in magnitude from $V = 10.94$ mag. to $V = 16.15$ mag. New photographic photometry based on these standards is given for 147 stars. The data have been then used to convert earlier photometry to the *BV* system for an additional 142 stars.

The color-magnitude diagram shows the giant (A), subgiant (B), asymptotic (C), and blue horizontal (D) sequences. The horizontal branch redward of the variable-star gap is absent as is characteristic of low metal-abundance clusters. Comparison of the M92 and M3 diagrams shows that the giant stars differ in intrinsic $B - V$ color between the two clusters as was suspected in earlier work.

The two-color diagram shows that the asymptotic branch C is clearly separated from the subgiant branch B in the $U - B$ index for both clusters. The difference in $U - B$ between branch C and B stars ranges from $\delta(U - B) = 0.08$ mag. to $\delta(U - B) = 0.37$ mag. read at constant $B - V$. This observed effect averages four times greater than is predicted by the change in emergent continuum flux caused by changing surface gravity in model atmospheres. Our observations could be explained if a presently unknown spectral absorption is present for stars on one branch but not on the other, causing a difference in the blanketing vectors which will separate the sequences in the two-color diagram. A possible explanation is that the emergent flux of branch B stars is decreased by about 10 per cent relative to C stars under the *B* photometric filter so as to give anomalous blanketing by 0.1 mag. in both $U - B$ and $B - V$, but a second less likely possibility is that branch C stars have a higher abundance of the heavy elements due to evolution through the giant phase.

I. INTRODUCTION

The present study of M92 was begun in 1955 to check the anomalous ultraviolet excess of stars in globular clusters which had been found the year before in NGC 4147 (Sandage and Walker 1955) and confirmed in M3 while the present work on M92 was in progress (Johnson and Sandage 1956). Various circumstances delayed publication of the results, and new data have been added to our original material during the past 10 years. By now it is well known that the ultraviolet excess is a general feature of all halo clusters, subdwarfs, and RR Lyrae stars, and is caused by the deblanketing effect of low metal abundance. However, accurate three-color photometry for a large number of globular clusters is clearly of importance, and this fact would in itself justify publication of the present material. In addition a new effect has been found in the $U - B$, $B - V$ diagram for stars on various sequences of the color-magnitude (C-M) diagram.

Our photometric material consists of three-color photoelectric measurements of 71 stars near M92 made with the 100- and 200-inch reflectors, together with photographic photometry for 147 stars based on four plates in each of the three colors.

II. THE PHOTOMETRIC DATA

The photoelectric colors and magnitudes for the seventy-one standard stars are given in Table 1, which is divided into two parts, showing (1) stars considered to be members on the basis of position in the C-M diagram, and (2) stars considered to be non-cluster members because of their scatter from the principal sequences together with their lack of

* Now at the Lick Observatory, University of California. Most of the work was done while the author was at the Mount Wilson and Palomar Observatories.

ultraviolet excess. The final column of the table indicates the sequence of the C-M diagram to which the particular star belongs. The notation of the sequences is shown later in Figure 3.

The stars in the first part of Table 1 are identified in Figure 1 using the numbering system adopted in an earlier study of the cluster (Arp, Baum, and Sandage 1953; hereafter called "Paper I"). These numbers are the same as used by Walker (1955), Deutsch (1955), and Helfer, Wallerstein, and Greenstein (1959) in their studies of special stars in this cluster. The identifications are given here for the first time.

Figure 2 gives the identification for stars of Table 1 in the extended neighborhood of M92, measured primarily to obtain the reddening of the cluster by the two-color method.

Table 2 shows the results of photographic photometry of 147 stars measured on plates taken with the 100-inch reflector diaphragmed to 58 inches. Four plates in each of the three colors were measured, and the results were corrected by means of small, non-linear color equations to the photoelectric *UBV* system defined by stars in Table 1. The plate and filter combination were U = 103aO + UG2; B = 103aO + GG13; and V = 103aD + GG11. The probable errors of the entries of Table 2 are about ± 0.02 mag. for V and $B - V$ and ± 0.04 mag. for $U - B$. Stars marked by asterisks in Table 2 are among the photoelectric standards of Table 1, and a comparison of the values in these two tables shows there is no remaining color or magnitude equation in the photographic data. Stars in this table are identified in Figure 1.

Table 3 gives two-color data for stars not included in the present program but which were measured in the initial work on the cluster (Paper I). These older data, on the m_{pg}, CI color system have been transformed to the V, $B - V$ system using color and magnitude equations derived from the stars in Table 2 which are common to both studies. The accuracy of the data of Table 3 is lower than for Table 2, with probable errors in B and V ranging from ± 0.04 to ± 0.07 mag. as explained in Paper I. The stars in Table 3 except for the central region are identified in Figure 1.

III. THE C-M DIAGRAM

Figure 3 shows the C-M diagram, where stars from Tables 2 and 3 are given as closed circles and crosses, respectively. The designation of the sequences A, B, C, and D is indicated. The smaller scatter of the closed circles about the sequences compared with the crosses is evident.

Comparison of Figure 3 with data from other clusters clearly shows that the shape of the C-M diagram of M92 differs from diagrams of clusters with higher metal abundances. The most striking difference is the way the asymptotic branch C approaches the region of the RR Lyrae star gap along a *sloping* path rather than along a true red horizontal branch. The presence or absence of a red horizontal branch is known to be a distinctive feature of cluster diagrams that is highly correlated with the metal abundance (Sandage and Wallerstein 1960). M92 is the finest example of a cluster which does not have a true red horizontal branch but which has a well-developed asymptotic sequence (C). Clusters with either intermediate or the opposite characteristics are M3 (Sandage 1953), NGC 6712 (Smith and Sandage 1962), NGC 6723 (Gascoigne and Ogston 1963), and NGC 6171 (Sandage and Katem 1964). In the last three cases, the red horizontal branches are well developed and the blue part of the horizontal branch is relatively weak.

Comparison of the diagrams of M92 and M3 is shown in Figure 4 where the present data for M92 and the older data for M3 have been used. Open circles and triangles are from Tables 1 and 5 of Johnson and Sandage (1956) and from recent, unpublished, measurements of the blue stars in M3. Closed circles are from Table 1 of this paper while closed triangles are normal points read from Figure 3 and listed in Table 4. The diagrams for M92 and M3 have been arbitrarily forced to coincide at the blue end of the horizontal branch and have been normalized along the ordinate for a distance modulus of $m - M$ = 14.62 mag. for M92 (Sandage 1964). A different procedure would have been to plot M3

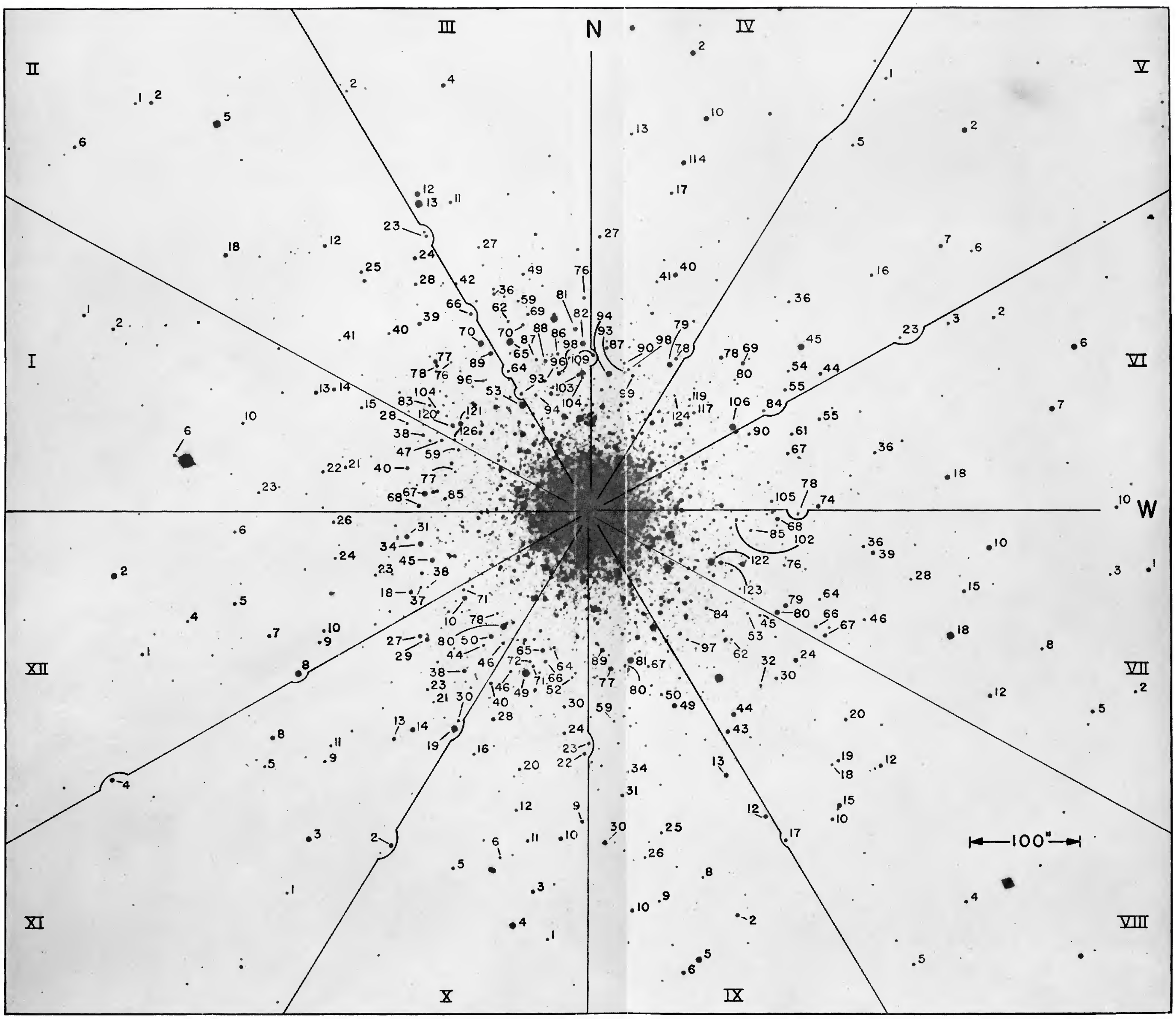

FIG. 1.—Identification chart for the stars in the immediate neighborhood of M92 listed in Tables 1–3. The print is from a 60-min exposure taken with the 100-inch reflector, diaphragmed to 58 inches, on 103a-D emulsion behind a Schott GG11 filter. The scale of the print is shown in the southwest corner.

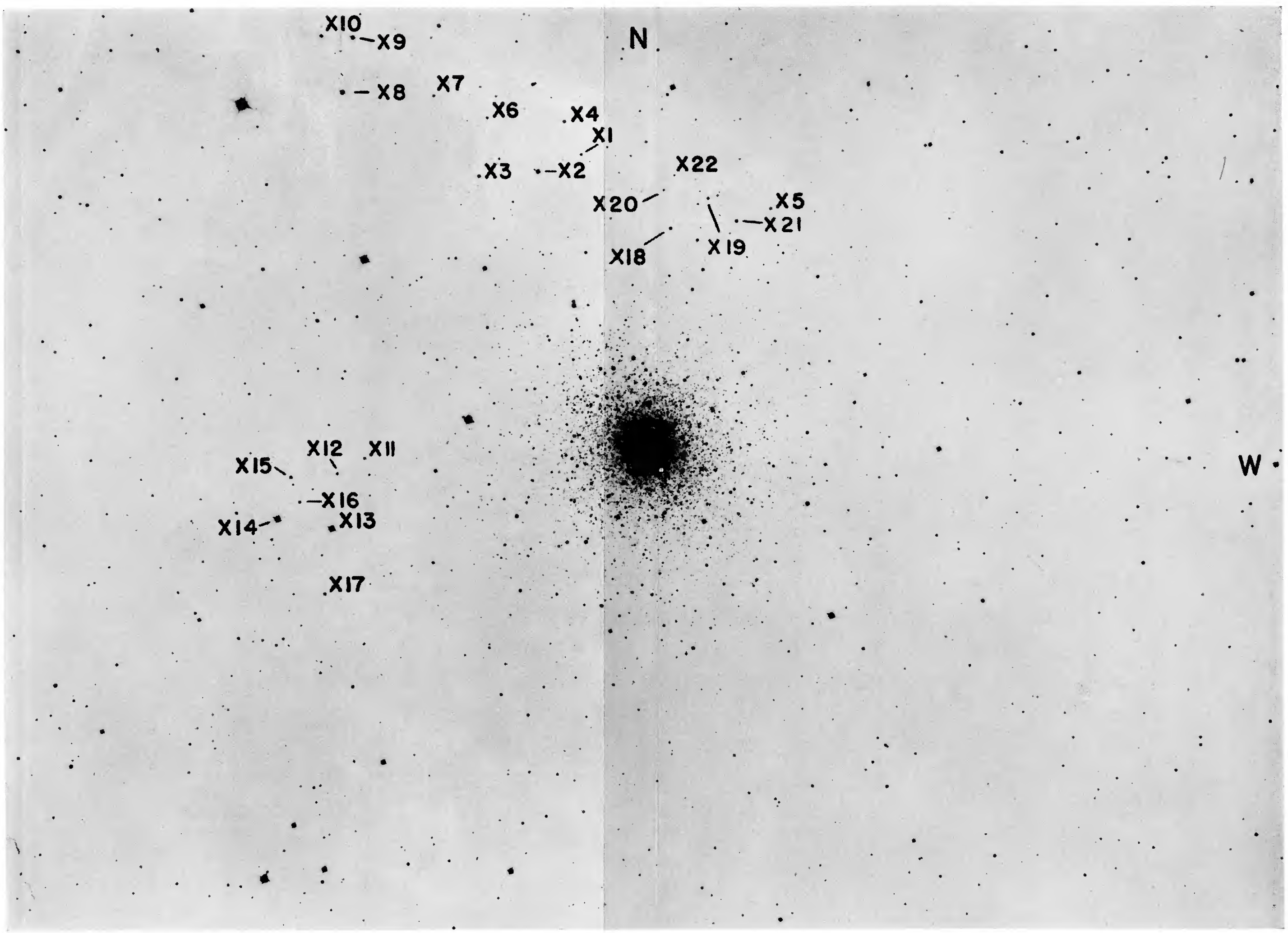

FIG. 2.—Identification of stars in the extended neighborhood of M92 whose magnitudes are given at the end of Table 1

TABLE 1

PHOTOELECTRIC OBSERVATIONS

Star	V	B − V	U − B	Members: n 200"	Members: n 100" or 60"	Branch
I-10	15.47	+0.02	+0.03	1	...	D
13	14.61	+0.52	−0.07	1	...	C
II-2	14.66	+0.57	−0.01	1	...	C
24	14.54	+0.78	+0.16	1	...	B
28	15.04	+0.44	−0.06	1	2	C
39	14.35	+0.70	−0.02	...	1	B
40	15.82	−0.08	−0.30	...	4	D
III-4	14.12	+0.71	+0.14	2	...	C
11	15.23	+0.69	+0.07	1	...	B
13	12.03	+1.33	+1.11	1	...	A
27	16.15	−0.12	−0.39	1	3	D
IV-2	13.52	+0.90	+0.43	2	...	A
10	13.42	+0.95	+0.45	18	2	A
13	15.38	+0.69	+0.09	1	...	B
17	15.51	+0.03	+0.02	7	...	D
27	15.20	+0.18	+0.11:	2	1	D
114	13.83	+0.87	+0.36	44	2	A
V-23	15.79	+0.02	−0.21	1	...	D
36	15.58	−0.02	−0.15	1	...	D
55	15.30	+0.16	+0.11	1	...	D
VI-3	15.33	+0.09	+0.09	1	...	D
10	15.24	+0.13	+0.10	...	4	D
18	13.73	+0.82	+0.30	1	...	A (C?)
55	15.25	−0.04	−0.03	1	...	D
61	15.31	+0.14	+0.12	1	...	D
VII-12	14.67	+0.72:	+0.17:	2	...	B
18	12.12	+1.31	+1.02	...	4	A
IX-12	14.52	+0.54	−0.06	...	2	C
XI-1	16.04	−0.04	−0.34	1	...	D
2	14.26	+0.73	+0.25	1	...	C (or B)
11	15.90	+0.02	−0.39	1	...	D
13	14.68	+0.51	−0.05	1	...	C
XII-1	15.11	+0.18	+0.08	...	2	D
6	15.84	−0.01	−0.15	1	...	D
8	12.76	+1.06	+0.57	...	5	A or C ?
24	15.94	−0.07	−0.19	2	...	D

Field Stars

Star	V	B − V	U − B	Members: n 200"	Members: n 100" or 60"
I-2	15.11	+0.82	+0.37	1	...
II-18	14.04	+0.92	+0.68	1	...
III-12	13.29	+0.77	.....	1	...
V-2	13.50	+1.05	+0.95	1	...
VI-2	15.45	+0.68	+0.21	...	2
6	13.16	+0.84	+0.35	...	3
7	13.54	+0.70	+0.11	...	3
74	14.25	+0.56	+0.07	1	...
VII-1	14.58	+0.89	+0.49	1	...
IX-5	13.09	+0.60	+0.05	1	...
X-4	12.81	+1.16	+1.04	...	5
XI-8	14.07	+0.59	+0.02	1	...
XII-2	12.89	+0.67	+0.09	...	5
× 1	14.94	+0.70	+0.27	...	1
× 2	12.27	+1.07	+0.98	...	1
× 3	13.32	+0.92	+0.71	...	1
× 4	13.54	+0.96	+0.66	...	1
× 5	14.22	+0.58	+0.03	...	1
× 6	14.96	+0.67	+0.18	...	1
× 7	15.06	+0.74	+0.32	...	1
× 8	11.96	+0.98	+0.61	...	1
× 9	12.48	+0.51	−0.02	...	1
× 10	14.05	+0.73	+0.29	...	1
× 11	14.43	+0.55	+0.02	...	1
× 12	14.22	+0.59	0.00	...	1
× 13	10.99	+0.77	+0.33	...	1
× 14	10.94	+0.40	0.00	...	1
× 15	13.46	+0.50	−0.09	...	1
× 16	14.40	+0.73	+0.22	...	1
× 17	14.30	+0.51	−0.08	...	1
× 18	13.35	+0.69	+0.25	6	...
× 19	14.24	+0.57	+0.03	...	2
× 20	15.68	+1.16	+1.05	2	...
× 21	13.64	+0.65	+0.16	4	...
× 22	15.47	+1.71	.....	1	...

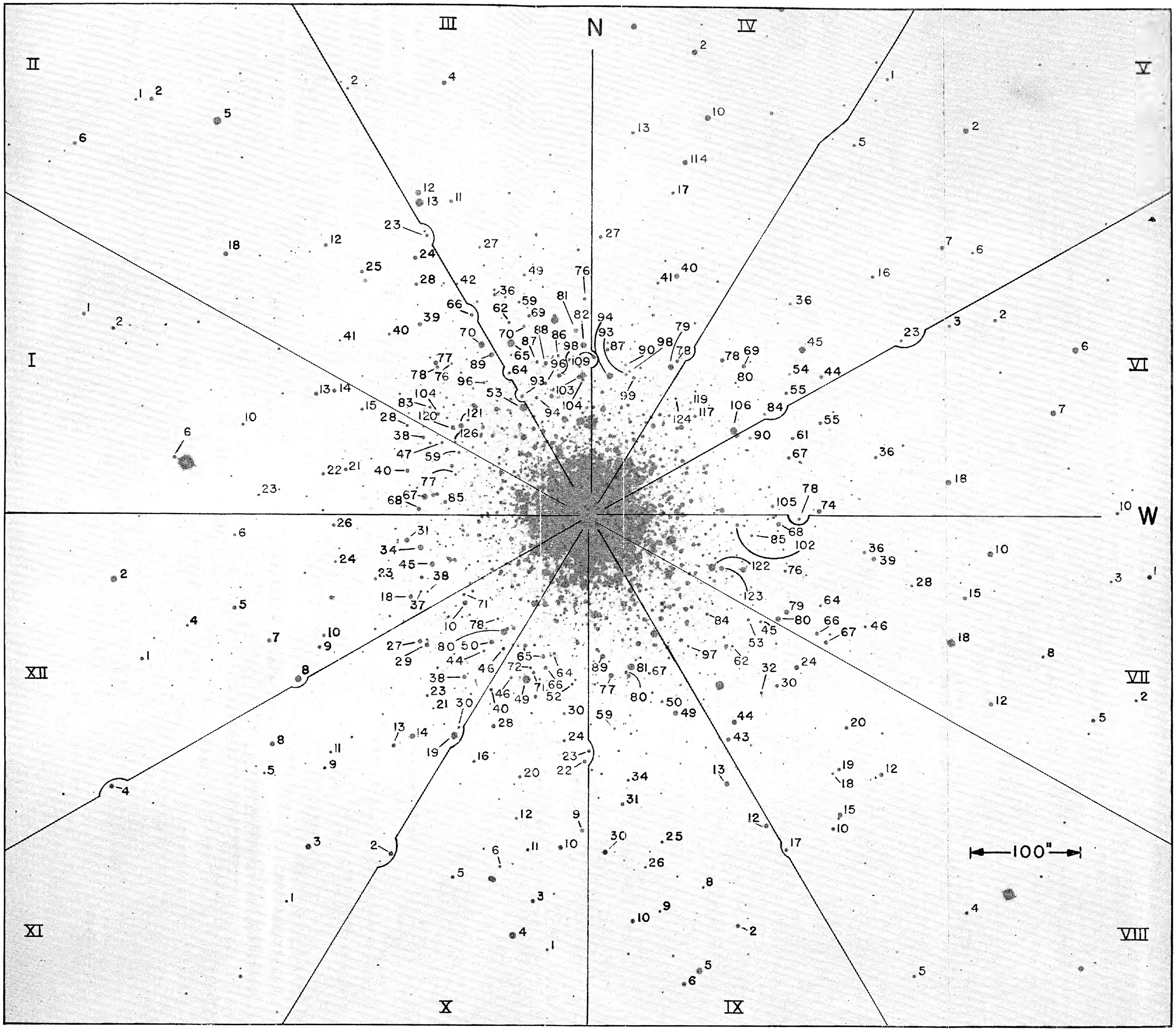

FIG. 1.—Identification chart for the stars in the immediate neighborhood of M92 listed in Tables 1–3. The print is from a 60-min exposure taken with the 100-inch reflector, diaphragmed to 58 inches, on 103a-D emulsion behind a Schott GG11 filter. The scale of the print is shown in the southwest corner.

TABLE 2

PHOTOGRAPHIC OBSERVATIONS

Star	V	B – V	U – B	Branch
I-1......	15.00	+0.63	+0.15	Field
2*.....	15.02	+0.88	+0.31	Field
10*.....	15.51	+0.01	+0.04	D
13*.....	14.62	+0.53	–0.12	C
14.....	14.74	+0.73	+0.12	B
21.....	15.23	+0.10	+0.12	D
22.....	15.31	+0.70	–0.09	B
28.....	15.65	–0.05	–0.15	D
38.....	15.15	+0.17	+0.08	D
40.....	14.78	+0.73	+0.14	B
47.....	15.51	+0.04	0.00	D
59.....	15.56	+0.02	0.00	D
67.....	13.32	+0.92	+0.55	A
II-2*.....	14.59	+0.60	–0.16:	C
6......	15.07	+0.73	–0.06	B
12.....	14.58	+0.77	+0.21	B
18*.....	14.03	+0.90	+0.70	Field
23.....	15.24	+0.13	+0.12	D
24*.....	14.54	+0.74	+0.19	B
25.....	15.27	+0.71	+0.09	B
28*.....	15.01	+0.48	–0.06	C
39*.....	14.34	+0.75	.....	B
40*.....	15.83	–0.05	–0.26	D
53.....	12.35	+1.18	+0.87	A
66.....	15.02	+0.09	+0.19	D
70.....	13.03	+0.98	+0.62	A
89.....	14.07	+0.74	+0.25	C
104.....	15.46	+0.68	–0.05	B
120.....	14.59	+0.74	+0.14	B
121.....	13.79	+0.71	+0.26	C
III-4*.....	14.12	+0.71	+0.11	C
11*.....	15.14	+0.76	+0.01	B
12*.....	13.29	+0.76	+0.47	Field
27*.....	16.06	–0.03:	–0.42	D
36.....	15.44	+0.71	–0.13	B
62.....	15.68	–0.09	–0.26	D
65.....	12.36	+1.18	+0.91	A
76.....	15.42	+0.70	–0.05	B
81.....	14.38	+0.59	+0.01	C
82.....	13.32	+0.94	+0.62	A
86.....	15.74	–0.01	–0.33	D
87.....	15.57	0.00	–0.08	D
96.....	15.08	+0.69	–0.03	B
IV-2*.....	13.49	+0.92	+0.51	A
10*.....	13.43	+0.94	+0.51	A
17*.....	15.50	+0.03	+0.02	D
27*.....	15.19	+0.16	+0.14	D
40.....	13.90	+0.73	+0.32	C
78.....	15.15	+0.18	+0.11	D
79.....	13.49	+0.90	+0.46	A
87.....	15.11	+0.74	+0.04	B
94.....	13.06	+0.96	+0.62	A
98.....	15.96	+0.04	–0.45	D
114*....	13.84	+0.83	+0.42	A
V-2......	13.48	+1.05	+0.90	Field
23*.....	15.87	+0.02	–0.24	D
36*.....	15.58	–0.07	–0.17	D
44.....	15.18	+0.72	+0.03	B
45.....	12.81	+1.03	+0.75	A
55*.....	15.28	+0.12	+0.14	D
69.....	14.60	+0.76	+0.07	B
78.....	14.48	+0.60	+0.11	C
106.....	12.47	+1.14	+0.79	A
VI-2*.....	15.58	+0.73	+0.08	Field
3*.....	15.34	+0.10	+0.05	D
6*.....	13.19	+0.79	+0.47	Field
7*.....	13.59	+0.66	+0.13	Field
10*.....	15.29	+0.17	+0.09	D
18*.....	13.76	+0.79	+0.29	C
55*.....	15.17	–0.03	+0.04	D
61*.....	15.28	+0.13	+0.12	D
67.....	15.14	+0.23	+0.11	D
74*.....	14.30	+0.50	+0.03	Field
VII-1*.....	14.51	+0.95	+0.43	Field
5......	14.99	+0.70	–0.05	B
10.....	13.71	+0.81	+0.33	C
12*.....	14.65	+0.75	+0.22	B
15.....	15.04	+0.74	+0.02	B
18*.....	12.14	+1.33	+1.01	A
36.....	15.38	+0.09	+0.08	D
39.....	14.48	+0.74	+0.15	B
46.....	15.81	–0.03	–0.19	D
66.....	15.09	+0.72	+0.02	B
67.....	14.70	+0.72	+0.11	B
68.....	14.26	+0.73	+0.26	C
79.....	14.21	+0.73	+0.29	C
80.....	13.92	+0.71	+0.24	C
122.....	12.29	+1.18	+0.87	A
VIII-4......	15.48	+0.60	–0.28:	B ?
12.....	14.76	+0.71	+0.13	B
15.....	14.28	+0.67	+0.25	C
17.....	15.28	+0.16	+0.13	D
18.....	16.11	+0.01	–0.42	D
19.....	15.36	+0.11	+0.04	D
20.....	15.22	+0.76	+0.01	B
24.....	14.14	+0.68	+0.18	C
43.....	14.62	+0.75	+0.12	B
44.....	14.13	+0.76	+0.33	C
IX-2......	14.69	+0.77	+0.16	B
5*.....	13.18	+0.55	+0.10	Field
6......	14.62	+0.76	+0.19	B
10.....	14.64	+0.74	+0.19	B
12*.....	14.51	+0.58	–0.03	C
13.....	14.02	+0.79	+0.35	A
30.....	14.13	+0.73	+0.29	C
49.....	13.90	+0.80	+0.39	C
77.....	14.19	+0.79	+0.26	B
81.....	12.92	+0.83	+0.62	Field
89.....	14.18	+0.74	+0.29	C
X-3......	14.63	+0.73	+0.18	B
4*.....	12.80	+1.15	+1.03	Field ?
5......	15.50	+0.04	0.00	D
9......	15.07	+0.61	–0.05	Field ?
10.....	14.38	+0.59	+0.01	C
22.....	15.13	+0.20	+0.08	D
23.....	15.40	+0.05	+0.12	D
24.....	15.47	+0.02	+0.05	D
28.....	14.62	+0.72	+0.15	B
49.....	12.16	+1.19	+1.10	A
65.....	14.34	+0.63	+0.08	C
XI-1*.....	16.07	+0.02	–0.49	D
2*.....	14.34	+0.66	+0.18	C
3......	13.56	+0.91	+0.46	A
4......	14.26	+0.66	+0.02	C
8*.....	14.13	+0.56	–0.02	Field ?
11*.....	15.90	–0.07	–0.34	D
13*.....	14.81	+0.52	–0.06	C
14.....	13.81	+0.85	+0.43	A
19.....	12.87	+1.05	+0.74	A
23.....	15.82	–0.03	–0.14	D
27.....	14.49	+0.66	+0.02	C
38.....	14.59	+0.76	+0.14	B
50.....	14.44	+0.88	+0.55	Field
70.....	14.11	+0.75	+0.29	C
XII-1*.....	15.12	+0.21	+0.06	D
2*.....	12.86	+0.64	+0.14	Field
5......	14.82	+0.74	+0.10	B
6*.....	15.79	–0.01	–0.14	D
7......	14.63	+0.75	+0.20	B
8*.....	12.74	+1.03	+0.78	A
9......	15.12	+0.15	+0.14	D
10.....	15.22	+0.15	+0.04	D
24*.....	15.89	–0.09	–0.19	D
26.....	15.27	+0.10	+0.12	D
31.....	13.97	+0.82	+0.36	A
34.....	13.46	+0.85	+0.49	C
45.....	14.08	+0.76	+0.32	C

*Stars with asterisks are among the photoelectric standards of Table 1.

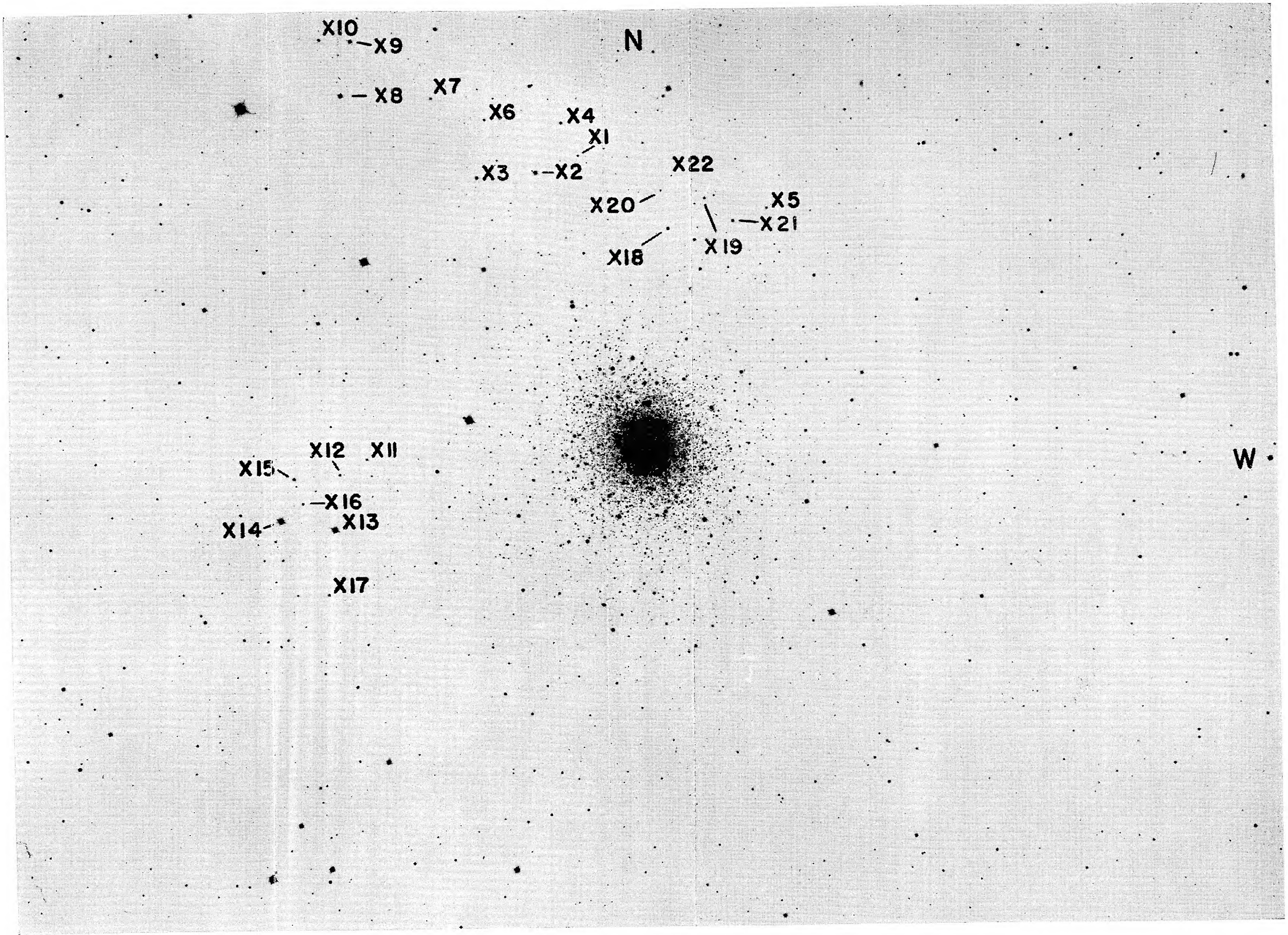

FIG. 2.—Identification of stars in the extended neighborhood of M92 whose magnitudes are given at the end of Table 1

TABLE 3

V, B − V VALUES CONVERTED FROM m_{pv},CI MEASUREMENTS

FOR STARS NOT IN TABLE 2

Star	V	B − V	Branch
I-6	15.35	+0.11	D
15	15.71	+0.69	B
23	15.97	+0.66	B
68	14.61	+0.75	B
77	16.02	−0.07	D
85	15.05	+0.71	B
II-1	15.77	+0.71	B
5	12.08	+0.83	Field
41	16.35	−0.07	D
76	16.24	−0.10	D
77	14.21	+0.74	C
78	15.36	+0.69	B
83	15.86	−0.05	D
96	15.98	+0.67	B
126	15.73	+0.71	B
III-2	15.92	+0.59	B
13	12.05	+1.46:	A
42	15.71	+0.71	B
49	15.63	+0.69	B
59	15.89	+0.67	B
64	15.77	+0.63	B
69	15.40	+0.71	B
70	15.54	+0.72	B
88	14.75	+0.72	B
93	15.18	+0.02	D
94	15.45	+0.72	B
98	14.50	+0.73	B
103	15.02	+0.12	D
104	13.46	+0.81	C or F
109	14.93	+0.72	B
IV-13	15.36	+0.66	B
41	15.95	+0.65	B
90	15.73	−0.02	D
93	15.85	0.00	D
99	15.12	+0.15	D
V-1	15.37	+0.64	B
5	15.69	+0.65	B
6	16.20	+0.62	B
16	15.47	+1.10	Field
54	15.86	+0.64	B
80	16.43	−0.09	D
84	15.66	+0.69	B
117	15.30	+0.05	D
119	16.04	+0.75	B
124	16.41	−0.07	D
VI-36	15.47	+0.71	B
78	15.83	+0.72	B
90	15.69	+0.72	B
105	15.64	+0.71	B
VII-2	15.81	+0.64	B

Star	V	B − V	Branch
VII-3	16.26	+0.68	B
8	15.81	+0.68	B
28	16.13	+0.67	B
64	16.09	+0.67	B
76	15.94	+0.70	B
85	15.80	−0.04	D
102	15.33	+0.06	D
123	14.32	+0.76	B or C
VIII-5	15.60	+0.90	Field
10	15.08:	+1.37:	Field
30	15.29	+0.04	D
32	16.08	−0.05	D
45	16.15	+0.68	B
53	16.06	+0.74	B
62	16.28	+0.01	D
84	15.72	+0.73	B
97	16.23	+0.74	B
IX-8	16.22	−0.08	D
9	15.97	+0.65	B
25	15.84	+0.64	B
26	16.28	−0.06	D
31	15.09:	+1.11	Field
34	16.03	+0.66	B
50	15.73	−0.08	D
59	16.33	−0.02	D
67	15.90	+0.73	B
80	15.02	+0.12	D
X-1	15.74	+0.62	B
6	16.09	+0.69	B
11	15.66	+0.64	B
12	16.03	+0.68	B
16	15.86	+0.65	B
20	15.61	+0.67	B
30	15.71	−0.01	D
40	15.58	+0.69	B
46	15.80	+0.70	B
52	16.09	+0.70	B
64	15.53	+0.01	D
66	15.05	+0.16	D
71	15.38	+0.10	D
72	15.94	+0.68	B
XI-5	16.23	+0.63	B
9	15.76	+0.87	Field
20	15.75	+0.76	B
21	16.30	−0.11	D
29	14.40	+0.62	C
44	15.93	+0.62	B
46	15.57	+0.76	B
71	15.79	+0.67	B
78	16.12	+0.04	D

Star	V	B − V	Branch
XI-80	13.04	+1.00	A
XII-4	15.89	+0.73	B
18	14.36	+0.72	C ?
23	15.61	+0.02	D
37	16.04	+0.73	B
38	16.27	−0.08	D
Central Region			
1	13.97	+0.74	A or C
2	14.50	0.66	C
3	13.94	0.87	A or F
5	12.35	1.26	A
6	13.96	0.72	C or A
8	13.84	0.82	A
10	13.11	1.04	A
11	13.88	0.76	A or C
12	14.40	0.72	B
13	13.13	0.93	A
15	12.55	1.10	A
16	13.50	0.75	F or C
19	13.59	0.94	A
20	12.97	0.81	Field
21	13.61	0.71	F or A
23	14.06	0.73	A or C
24	12.19	1.30	A
25	12.76	1.01	A
26	13.75	0.77	C or A
27	13.49	0.94	A
31	12.51	1.12	A
32	13.95	0.73	C
33	13.90	0.73	C
34	14.21	0.73	B
35	11.99	0.96	Field
36	14.28	0.71	B or C
37	14.38	0.74	B
38	12.53	1.11	A
39	12.39	1.12	A
40	12.39	1.22	A
44	13.90	0.71	C
54	12.15	1.17	A
58	11.95	1.16	Field ?
61	12.17	1.36	A
62	12.14	1.32	A
72	12.97	+0.94	A

*There is no identification chart available for stars in the central region.

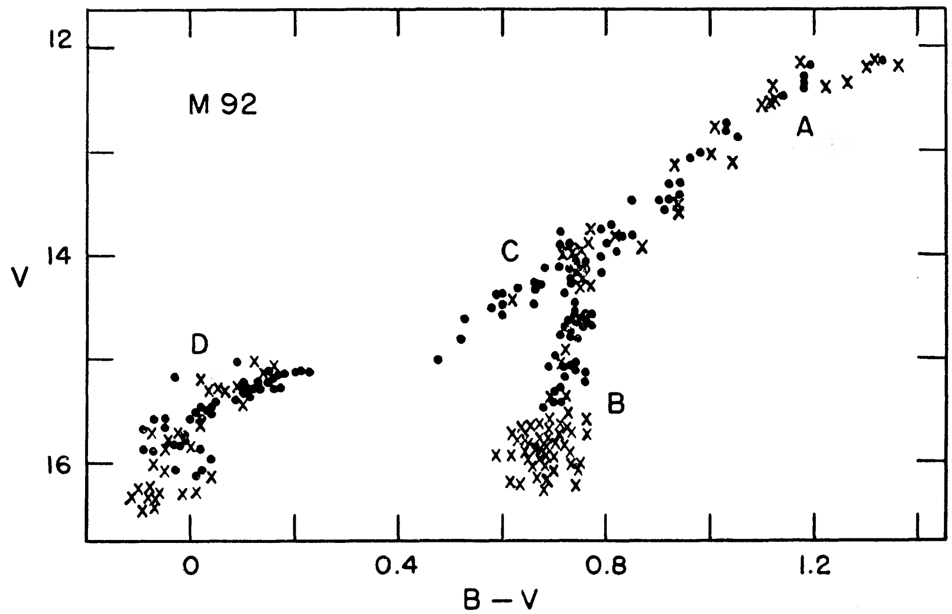

FIG. 3.—The color-magnitude diagram from the data of Tables 2 and 3. The closed circles are data from the present study in Table 2. The crosses are earlier data transformed to the BV system as given in Table 3. The four sequences are designated by letters A, B, C, and D.

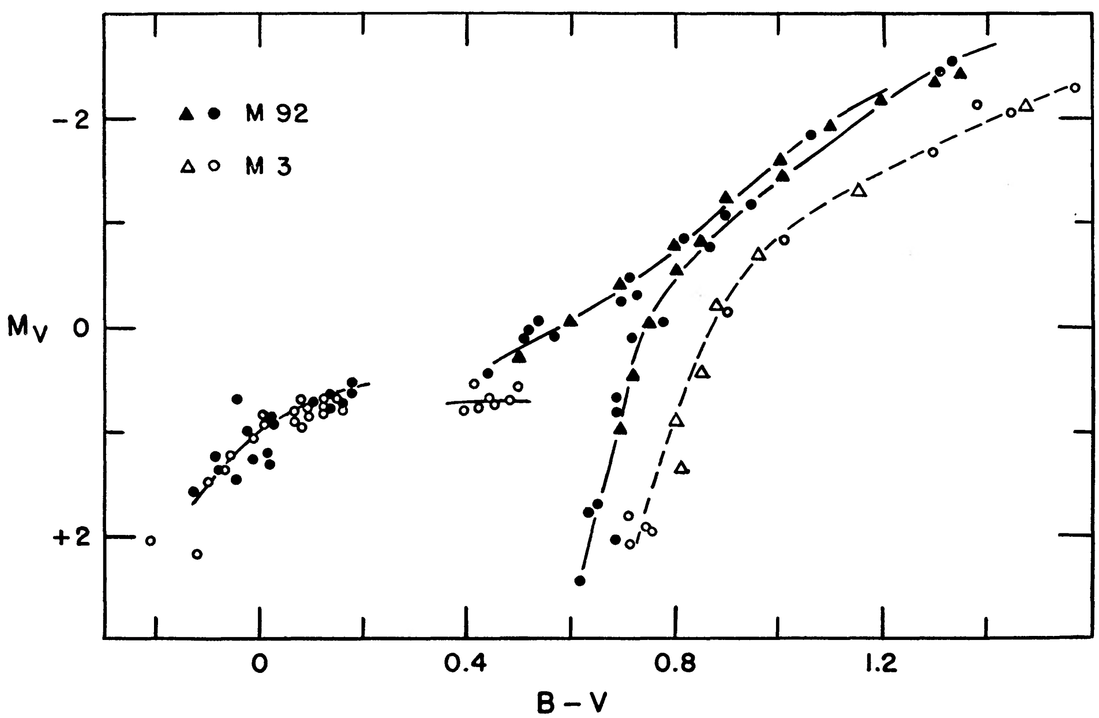

FIG. 4.—Comparison of the color-magnitude diagrams of M92 and M3. The blue ends of the horizontal branches have been arbitrarily superposed in magnitude. No shift along the $B - V$-axis has been made. The absolute-magnitude scale is that of M92 obtained by assuming $m - M = 14.62$ mag.

independently of such normalization at a modulus of $m - M = 15.40$ mag. determined from the main-sequence fit (Sandage 1964) and let the horizontal branches fall where they will in Figure 4. This would have separated the horizontal blue branches by about 0.4 mag., M3 being brighter.

The accuracy of the data on distances provides no choice between the two procedures, each being equally probable because the estimated errors of $m - M$ from the main-sequence fitting method is at least ± 0.20 mag. due to errors in the blanketing corrections and in the position of the observed main sequences themselves. We prefer the interpretation of Figure 4 because it agrees with the composite C-M diagram for all globular clusters (Tifft 1963, Fig. 2; Sandage 1965), constructed by properly matching the observed main sequences to the Hyades (with allowance for blanketing), which shows a progressive color displacement of the giant branch with metal abundance. It is possible that the main-sequence fitting of M3 (i.e., the alternative to Fig. 4) does not give the correct answer because of remaining small errors in the color of the faintest main-sequence stars

TABLE 4

ESTIMATED NORMAL POINTS FOR M92

Branches A and B		Branches C and D	
V	$B-V$	V	$B-V$
12.11	1.35	12.93	+1.00
12.18	1.30	13.35	+0.90
12.34	1.20	13.77	+0.80
12.62	1.10	14.14	+0.70
13.06	1.00	14.49	+0.60
13.51	0.90	14.85	+0.50
13.73	0.85	15.14	+0.23
14.00	0.804	15.30	+0.10
14.50	0.75	15.43	+0.05
15.00	0.72	15.65	0.00
15.50	0.698	16.00	−0.05
16.00	0.68	16.40	−0.09

in that cluster (Sandage 1964). If the comparison shown in Figure 4 is correct, we see immediately that the colors of the giant and subgiant branches differ between the clusters as suspected from earlier work (Arp, Baum, and Sandage 1952; Baum 1952). There are at least two mechanisms known to be operating which can cause the color difference. These are (1) differences in chemical composition between the clusters producing differential line blanketing on the $B - V$ colors, and (2) real differences in the position of the sequences in the M_{bol}, log T_e-plane due to a change in radius as a function of metal abundance (see Hoyle and Schwarzschild 1955, Fig. 4). (Differential interstellar reddening can be eliminated because $E_{(B-V)} = 0.00$ for M3 [Sandage 1964] and $E_{(B-V)} = 0.01$ for M92 [Sandage 1964]. Correction of the colors for reddening has not been applied for M92 because it is 0.00 mag. to the precision of the determination.)

Mechanism (1) must produce some effect because it is known that M92 has considerably weaker lines than M3 (Morgan 1956, 1959; Deutsch 1955; Kinman 1959). It is unknown at present whether this can explain the entire effect because blanketing vectors for giants have not yet been determined. The second effect is known to be present in other clusters and is most clearly seen in the comparison of 47 Tuc, NGC 188, and M67 (Wildey 1961, Fig. 4; Tifft 1963, Fig. 2). Here the giants in metal-rich clusters such as NGC 188 are at least 2 magnitudes fainter at $(B - V)_0 = 1.4$ mag. than stars in the metal-poor globular clusters in comparable evolutionary stages. This cannot be due to differential line blanketing because the difference is much too great. It seems likely, therefore, that part of the difference shown in Figure 4 is real and is due to the effect of the chemical composition on the stellar structure.

To separate the blanketing and radius effects observationally will require that M3 and M92 be observed on a green-red-infrared color system such as $(G - R)$, $(R - I)$ where the blanketing effect is known to be close to zero (Sandage and Smith 1963). Any color difference which then exists between C-M diagrams on an $R - I$ system will be due to the radius change alone.

IV. THE $U - B$, $B - V$ DIAGRAM

The two-color diagram, taken from the data of Table 2, is shown in Figure 5. The giant and subgiant branches A and B show the well-known ultraviolet excess relative to the Hyades main sequence (shown as a continuous solid line).

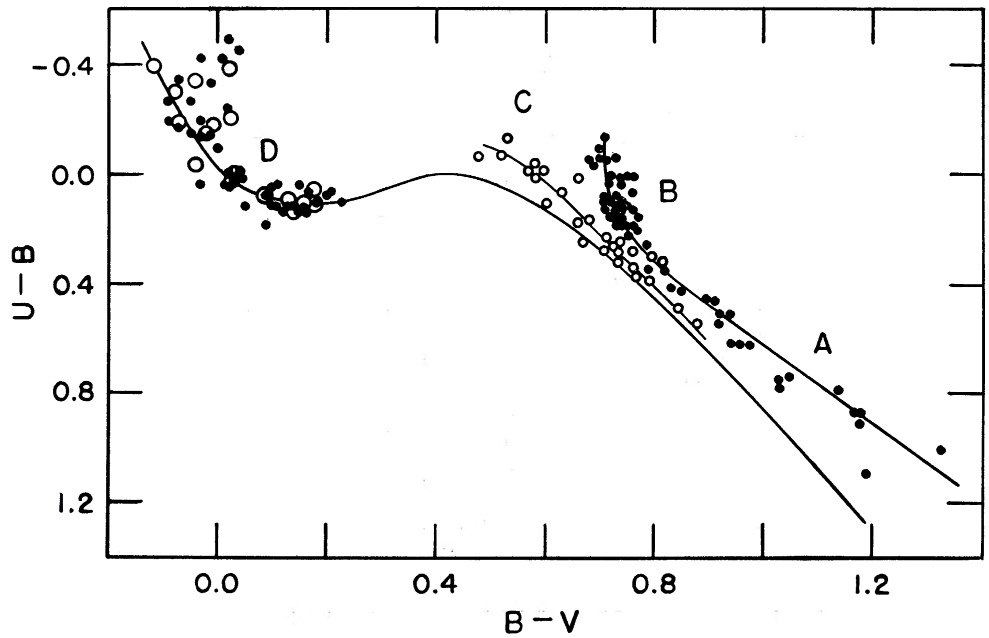

FIG. 5.—The two-color diagram taken from the data of Table 2. Large open circles on sequence D are photoelectric values from Table 1. The standard main-sequence relation is shown for comparison. The designation letters are the same as in Fig. 3.

Stars on the horizontal branch D show no excess or deficiency in $U - B$ relative to the standard sequence until $U - B \simeq -0.2$ mag., at which point the observed sequence bends toward redder $B - V$ values. The reality of the break at $U - B = -0.2$ mag. depends on two photoelectric standards (XI-1, and XI-11) observed only once, and we do not consider the result to be established. Furthermore, the bend cannot be understood theoretically because the results of Mihalas (1965, Figs. 8 and 10) show that the $U - B$, $B - V$ diagram is virtually independent of log g in this temperature range. Moreover, the effect does not occur in other globular clusters (Arp 1962, for M5; Sandage, unpublished for M13 and M15; Fig. 9 of this paper for M3). We therefore suspect the photometry of XI-1 and XI-11 and hold the result in reserve.

The most interesting feature of Figure 5 is the separation of the asymptotic branch C, shown as open circles, from the subgiant sequence B. Apparently, stars on sequences B and C can be separated on the basis of broad-band colors alone. The separation amounts to 0.08 mag. in $U - B$ at $B - V = 0.8$ mag. and increases toward bluer colors. This feature is strong independent evidence for the *existence* of the asymptotic branch which heretofore has been split into a separate sequence only on the basis of the C-M diagram alone (Sandage 1953; Arp 1955).

To study the effect more closely, we show in Figures 6 and 7 a part of the C-M and two-color diagrams where only the data in Table 2 are used. Stars assigned to branch C from the C-M diagram alone are given in Figure 6 as circles. The box incloses stars with $0.77 \geq B - V \geq 0.68$. These are analyzed in a special way later in this section. This same box is shown in Figure 7 which is an enlarged portion of Figure 5. Note the clean separation of branches B and C.

The same effect is present and indeed was first detected (Walker 1965) in the published observations of M3 (Johnson and Sandage 1956) but, because of the lower accuracy of the data, is somewhat less pronounced. Figure 8 shows the C-M diagram taken from

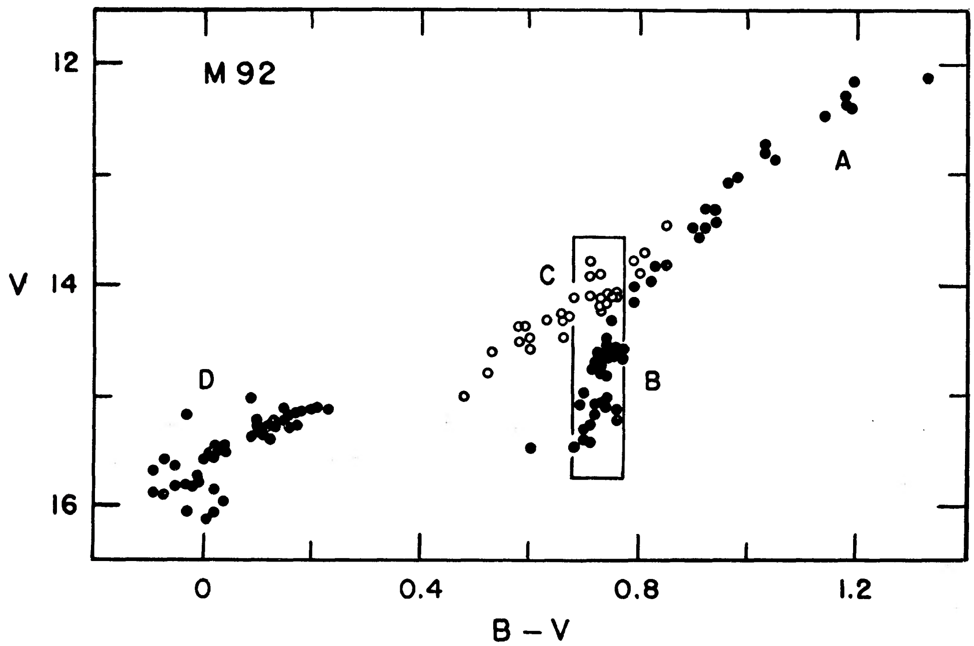

FIG. 6.—The color-magnitude diagram using only the stars in Table 2. The stars on the asymptotic branch C are shown by open circles to emphasize the separation from branches A and B. The box incloses stars with $0.77 \geq B - V \geq 0.68$ used for a study of $\delta(U - B) = f(V)$ in Fig. 10.

Johnson and Sandage (1956, Table 3). The coding of the points is as follows: stars assigned to branch C on the basis of Figure 8 alone are shown by open circles; stars on the true red horizontal branch by crosses; stars previously believed to be non-members (AT, II-12, II-43, III-32, and IV-7) but now considered to be cluster members by the argument given below by X; and branches A, B, and D by closed circles. The position of these stars in the two-color diagram is shown in Figure 9, using the same coding. Again, the open circles are closer to the Hyades line than are the closed circles, while the crosses appear to be intermediate.

The effect is conveniently summarized in Figure 10 where the ultraviolet excess, $\delta(U - B)$, of each star within the boxes of Figures 6–9 is correlated with the V magnitude in M3 and M92. The excess is defined, as usual, as the difference between the Hyades standard relation and the observed $U - B$ read at the observed $B - V$. The systematic trend in Figure 10 seems to be beyond doubt. The fact that the five crosses in M3 follow the trend argues that these stars are members of the cluster and therefore that the red end of the horizontal branch probably extends almost to the subgiants in M3.

The size of the effect is $\delta(U - B)/\Delta V \simeq 0.24$ mag. in M92 and 0.17 mag. in M3 which

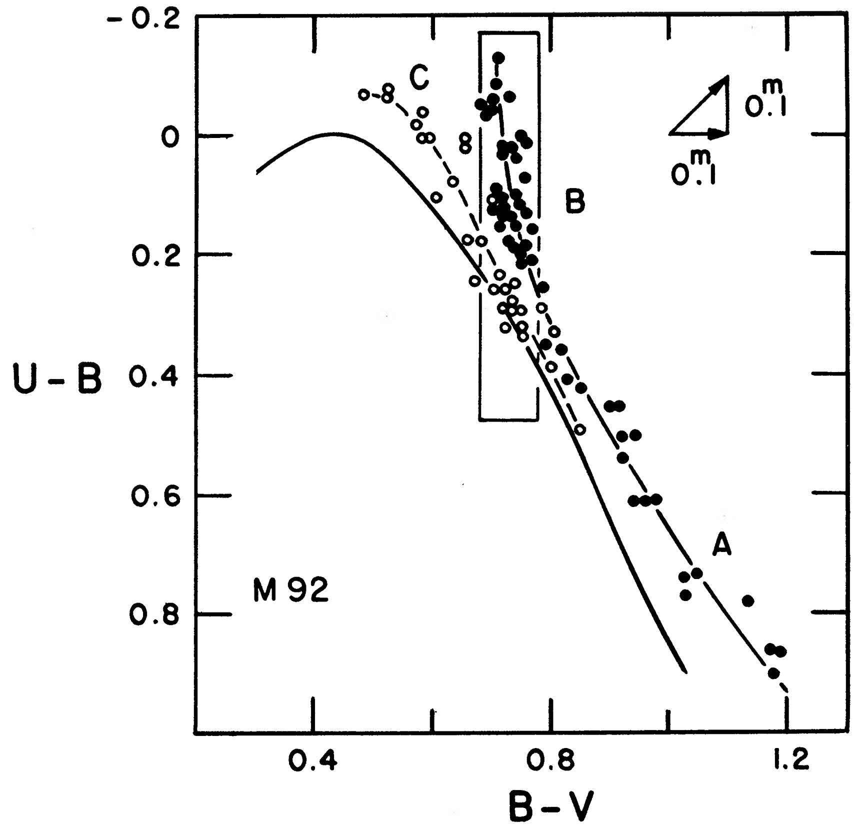

FIG. 7.—Enlarged view of Fig. 5 showing the larger ultraviolet excess of branch B stars compared with branch C. Differential blanketing vectors of 0.1 mag. in both $B - V$ and $U - B$, caused by a 10 per cent additional absorption under the photometric B filter in branch B stars, are shown.

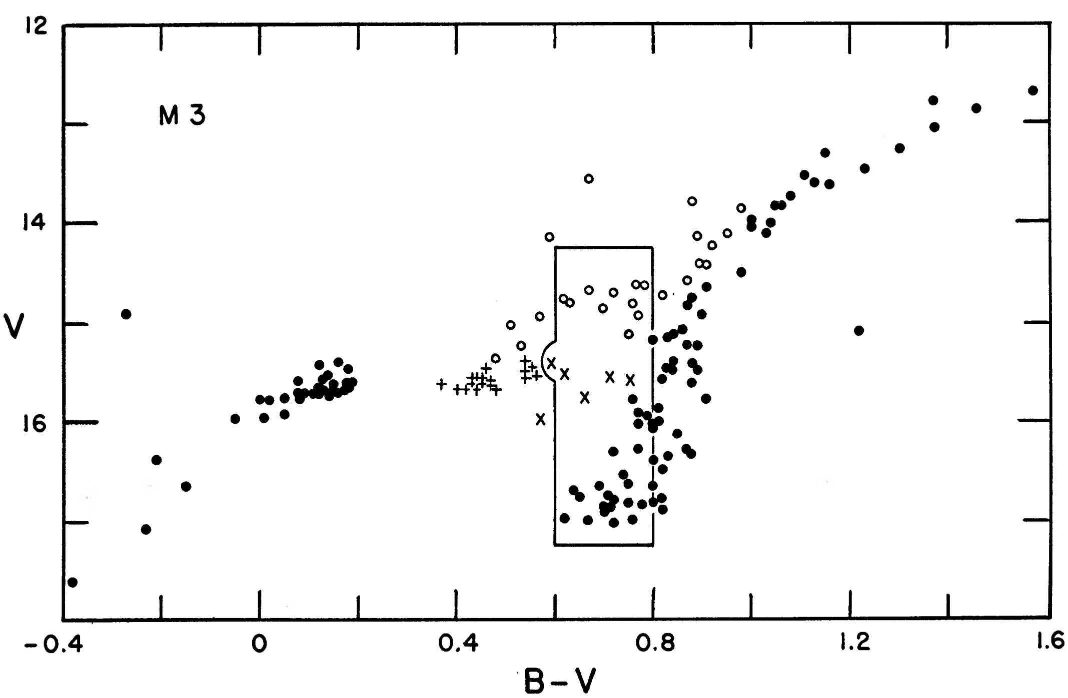

FIG. 8.—The color-magnitude diagram for M3 taken from data in the literature. The coding is explained in the text. Stars inclosed in the box with $0.80 \geq B - V \geq 0.60$ are those shown in Fig. 10.

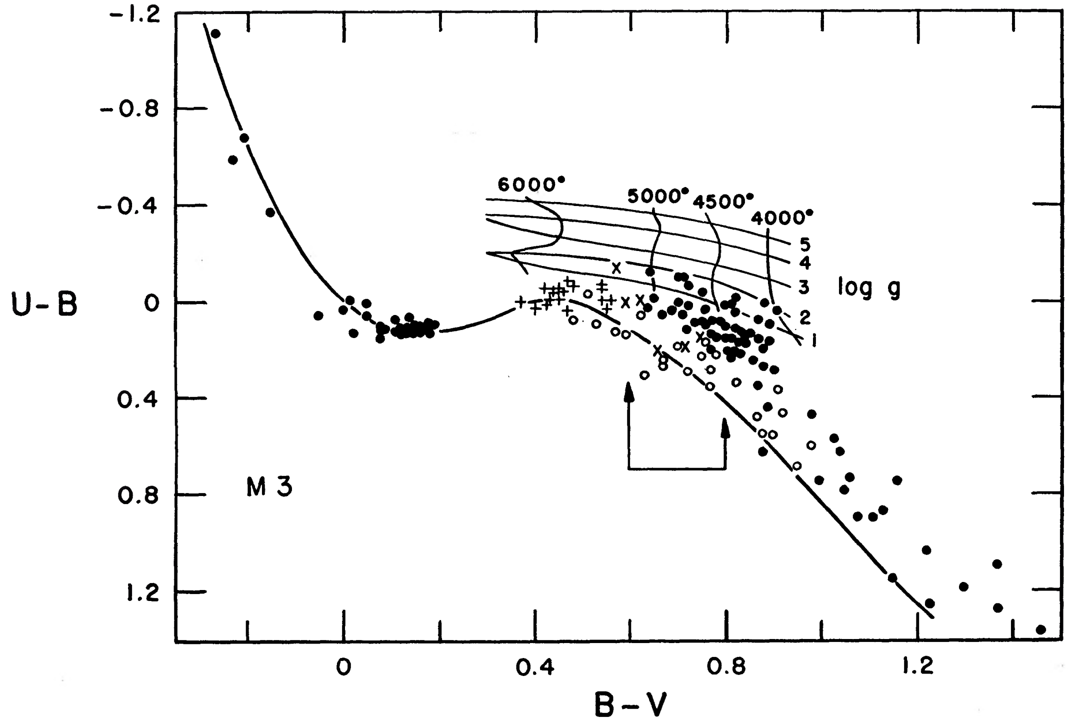

FIG. 9.—The two-color diagram for M3 with the same coding as Fig. 8. The grid represents the position of the line-free atmospheric models of De Jager and Neven for different values of log g and T_e. The data redder than $B - V = 0.4$ mag. are photographically determined. Bluer than $B - V = 0.4$ mag. the data are photoelectric from unpublished work by Sandage.

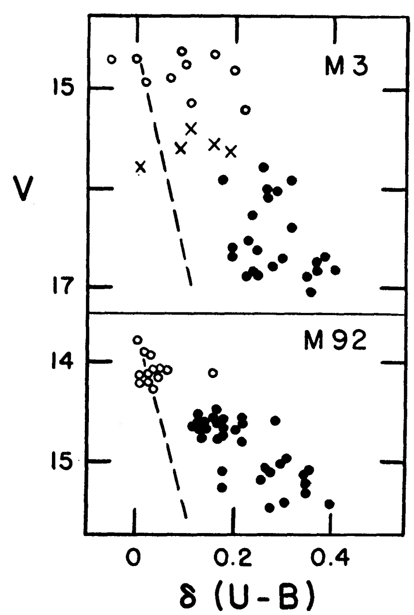

FIG. 10.—The change of the ultraviolet excess with apparent V magnitude for stars inclosed in the boxes of Figs. 6–9. Branch C stars are open circles. Branch B stars are closed circles. The dashed lines show the prediction of the effect of differing surface gravity in stars where *differential* line blanketing between branch B and C stars is zero and where no mass loss occurs between the branches. The observed slope violates the prediction by a factor of about 4.

is about four times that which can be explained by the effect of the difference of surface gravity (electron pressure) on the emergent continuum flux between stars on the B and C branches.

The gravity effect can be predicted by three different methods. (1) Emergent continuum fluxes for model stars of different log g and T_e have been computed by De Jager and Neven (1957), among others. We have calculated continuum $U - B$, $B - V$ colors for these models using equations given elsewhere (Matthews and Sandage 1963, Appendix A), and the results, slightly smoothed, are shown in Figure 9 for the color range of interest. Interpolating in this graph at $B - V = 0.7$ mag. gives $\delta(U - B)/\Delta \log g = 0.08$ mag. The danger of using this result as it stands lies, of course, in the neglect of the lines. Because the Fraunhofer lines become stronger at a given $B - V$ as log g increases (going from giants to dwarfs) the value of 0.08 mag. is expected to be an underestimate because the spacing of the loci of constant log g in Figure 9 will increase due to the increased blanketing for higher values of log g .This expectation is borne out by the following independent estimates where the lines are taken into account. (2) Eggen's calibration of the absolute-magnitude effect on $\delta(U - B)$ in the range 0.6 mag. $\geq B - V \geq 0.2$ mag. using double stars, one component of which has evolved (Eggen 1963; Eggen and Sandage 1964, Fig. 5) gives $\delta(U - B)/\Delta \log g = 0.13$ mag. where the difference in the g-values for the stars involved is calculated from the usual radius and mass relations. (3) The surface-gravity effect between dwarfs and supergiants, summarized in Figure 4 of a previous paper (Eggen and Sandage 1964), shows that the difference between $U - B$ values of luminosity class Iab and V stars is 0.32 mag. at $B - V = 0.65$ mag. The difference of log g-values is about 2.9 ($\log g_{\rm V} = 4.4$, $\log g_{\rm Iab} \simeq 1.5$) which gives $\delta(U - B)/\Delta \log g = 0.11$ mag.—a value which is consistent with the other estimates. We shall adopt a value of 0.12 mag. in the following.

To estimate how much branches B and C should differ in $U - B$ from the gravity effect alone we must calculate $\Delta \log g$ between the sequences. Quite generally

$$\log \frac{g_{\rm B}}{g_{\rm C}} = \log \frac{L_{\rm C}}{L_{\rm B}} + 4 \log \frac{T_{\rm B}}{T_{\rm C}} + \log \frac{M_{\rm B}}{M_{\rm C}} . \tag{1}$$

The stars in Figure 10 have been taken from a narrow range of $B - V$ which means to a first approximation that $T_{\rm B} \simeq T_{\rm C}$ if the line-blanketing effects are the same for both sequences. Equality of T_e for a given $B - V$ follows because the lines of constant T_e are nearly vertical in Figure 9. If we further assume the masses are equal on the B and C branches, and that the bolometric corrections are the same for equal $B - V$, then

$$\Delta \log g = 0.4(V_{\rm B} - V_{\rm C}) , \tag{2}$$

where V_i is the apparent visual magnitude on branch i.

Adopting $\delta(U - B)/\Delta \log g = 0.12$ mag. for the gravity effect predicts from equation (2) that

$$\frac{\delta(U-B)}{\Delta V} = 0.048 . \tag{3}$$

Equation (3) is shown in Figure 10 as a dotted line. The inadequacy of the surface-gravity explanation is evident from the lack of agreement of this line with the plotted points. The discrepancy is real because calculation shows that the neglect of the small variation in $B - V$ of the stars in Figure 10, which neglects the variation of T_e in equation (1), does not change the result. Likewise, a change of mass between stars of branches B and C cannot be invoked because the impossibly large mass ratio of $\mathfrak{M}_B/\mathfrak{M}_C = 30$ would be required. The results, therefore, rule out a gravity effect per se as the explanation of Figures 7, 9, and 10.

We are now forced to conclude that a difference in line or continuous absorption exists between at least groups C and B, and possibly within group B as well, in M92 and M3. The absorption required to explain Figure 10 could be either: (1) line or continuous absorption under the *B* band amounting to 10 per cent (0.1 mag.) in integrated effect over the 1200-Å pass band of the filter, or (2) line or continuous absorption amounting to 0.2 mag. under the *U* filter. Absorption by a single line or band, such as, e.g., the *G* band due to the CH molecule, can be ruled out since to produce the observed effect a change in intensity of a feature 100 Å wide from 0 to 100 per cent would be required. Image-tube spectra (dispersion 48 Å/mm) with the coudé spectrograph of the 120-inch Lick reflector have been obtained for several pairs of stars from sequences B and C and show that no such obvious effect exists. Thus, we are forced to conclude that there is a change in the continuous absorption in the blue or ultraviolet, or that a change in the strengths of all of the (metal) absorption lines occurs. A decision as to which of these mechanisms is correct will probably only be possible after high-dispersion spectra of stars in groups B and C are obtained and equivalent widths measured, or by making differential narrow-band photoelectric measurements of stars on both branches.

It might be imagined that the difference between branch B and C stars could be caused by a difference in metal abundance. However, if this were so, the points in Figure 10 would have to have a slope within each group equal to the theoretical gravity line shown in that diagram. We cannot exclude that possibility in M3, but in M92 where the data are more accurate, the slope of the points appears to deviate significantly from the gravity line, which indicates that, if a chemical composition difference is the explanation, this difference must act along branch B itself. Differences in chemical composition along a given branch seem unreasonable in light of our present knowledge, and we have no explanation for the effect at this time. Nevertheless it is interesting to speculate that, if branch B stars are normal and if only a simple discontinuity had existed between branches B and C, each satisfying the gravity line, this result might have arisen from an enrichment in the metal content of the group C stars. This enrichment might be brought about if these objects represent stars which have passed through the extreme red-giant phase, at which time very deep convection extending nearly to the center of the star occurs that might bring up material from the core, where the metal content is higher because of nuclear processes.

REFERENCES

Arp, H. C. 1955, *A.J.*, **60**, 317.
———. 1962, *ibid.*, **135**, 311.
Arp, H. C., Baum, W. A., and Sandage, A. R. 1952, *A.J.*, **57**, 4.
———. 1953, *ibid.*, **58**, 4 (Paper I).
Baum, W. A. 1952, *A.J.*, **57**, 222.
Deutsch, A. J. 1955, *Principes fondamentaux de classification stellaire* ("Colloq. Internat. Centre Natl. Rech. Sci.," Paris), p. 25.
Eggen, O. J. 1963, *A.J.*, **68**, 697.
Eggen, O. J., and Sandage, A. R. 1964, *Ap. J.*, **140**, 130.
Gascoigne, S. C. B., and Ogston, F. A. 1963, *Observatory*, **83**, 64.
Helfer, H. L., Wallerstein, G., and Greenstein, J. L. 1959, *Ap. J.*, **129**, 700.
Hoyle, F., and Schwarzschild, M. 1955, *Ap. J. Suppl.*, **2**, 1.
Jager, C. de, and Neven, L. 1957, *Ann. Obs. R. Belg.*, Vol. **8**.
Johnson, H. L., and Sandage, A. R. 1956, *Ap. J.*, **124**, 379.
Kinman, T. D. 1959, *M.N.*, **119**, 538.
Matthews, T. A., and Sandage, A. R. 1963, *Ap. J.*, **138**, 30.
Mihalas, D. 1965, *Ap. J. Suppl.*, **9**, 321 (No. 92).
Morgan, W. W. 1956, *Pub. A.S.P.*, **68**, 509.
———. 1959, *A.J.*, **64**, 432.
Sandage, A. R. 1953, *A.J.*, **58**, 61.
———. 1964, "Ann. Rept. Mt. Wilson Obs.," *Carnegie Inst. of Wash. Yrbk.*, No. 63 p. 23.
———. 1965, in preparation.

Sandage, A. R., and Katem, B. 1964, *Ap. J.*, **139**, 1088.
Sandage, A. R., and Smith, L. L. 1963, *Ap. J.*, **137**, 1057.
Sandage, A. R., and Walker, M. F. 1955, *A.J.*, **60**, 230.
Sandage, A. R., and Wallerstein, G. 1960, *Ap. J.*, **131**, 598.
Smith, L. L., and Sandage, A. 1962, *A.J.*, **67**, 121.
Tifft, W. G. 1963, *M.N.*, **126**, 209.
Walker, M. F. 1955, *A.J.*, **60**, 197.
———. 1965, Paper given at NASA Conference on Stellar Evolution, Goddard Space Sci. Lab., Nov. 1963 (in press).
Wildey, R. L. 1961, *Ap. J.*, **133**, 430.